Electronic Supplementary Material (ESI) for New Journal of Chemistry.

Supporting Information

Synthesis of Bz-TTFs with Polymerization Sites and Properties of Li-ion Batteries Comprising them as Active Materials

Aya Yoshimura,[a] Moeko Yoshinouchi,[a] Keisuke Hemmi,[a] Yuto Aso,[a] Ryosuke Utsumi,[a] Takashi Shirahata,[a,b] Masaru Yao,[c] and Yohji Misaki*[a,b]

[a] *Department of Applied Chemistry, Graduate School of Science and Engineering, Ehime University 3 Bunkyo-cho, Matsuyama 790-8577 (Japan)*

[b] *Research Unit for Development of Organic Superconductors, Ehime University 2-5 Bunkyo-cho, Matsuyama 790-8577 (Japan)*

[c] *Research Institute of Electrochemical Energy, National Institute of Advanced Industrial Science and Technology (AIST), 1-8-31 Midorigaoka, Ikeda, Osaka 563-8577 (Japan)*

Table of Contents

General Comments

All manipulations were performed under an argon atmosphere and all reagents were purchased from commercial suppliers and used without further purification. ^{1}H and ^{13}C NMR spectra were recorded on a Bruker Biospin AVANCE 400 or Bruker Biospin AVANCE III 500 spectrometer equipped with a CryoProbe (400 MHz for ^{1}H and 126 MHz for ^{13}C) using Acetone-d_6-CS_2 or C_6D_6-CS_2 solvent. The chemical shifts were referenced to tetramethylsilane for ^{1}H and ^{13}C NMR or the solvent resonances for ^{13}C NMR as internal standards (C_6D_6: 128.060 ppm). The high-resolution mass spectra were recorded on Thermo Scientific, Exactive Plus Orbitrap Mass Spectrometer for electrospray ionization (ESI). Melting points were determined with a Yanaco MP-500D. IR spectra were recorded on a JASCO FT/IR-460 plus spectrometer. The elemental analyses were determined by MICRO CORDER JM10T.

The diffraction data of **1** and **2** were collected on a Rigaku VariMaxSaturn724 CCD system at the Advanced Research Support Center, Ehime University using multi-layer mirror monochromated Mo-Kα radiation. Raw frame data were integrated using CrysAlisPro[1] and the data were corrected for Lorentz and polarization effects. The crystal structures were solved by the dual-space method (SHELXT-2018/2)[2] and refined by full-matrix least squares on F^2 (SHELXL-2018/3).[2,3]

The powder X-ray diffraction (XRD) patterns were collected on a Rigaku MiniFlex II diffractionmeter using Cu$K\alpha$ radiation.

Cyclic voltammetries (CV) were recorded on ALS/chi 617B Electrochemical analyzer. The CV cell consisted of Pt working electrode, Pt wire counter electrode, and an $Ag/AgNO_3$ reference electrode. The measurements were carried out in benzonitrile and carbon disulfide-benzonitrile solution (1:1, v/v) with a concentrate 0.1 M $^{n}Bu_4N^{+}PF_6^{-}$ as a supporting electrolyte with a scan rate of 50 mV s^{-1} at 25 °C. All redox potentials were measured against Ag/Ag^{+} and converted to vs. Fc/Fc^{+}, where Fc denotes ferrocene.

The cell performance was examined using the R2032 type cell composed of a positive electrode incorporating **1** and **2**, and a negative electrode using a lithium metal sheet. The positive electrode was prepared by mixing of active material, acetylene black as the conductive additive, and poly(tetrafluoroethylene) as the binder. The weight ratio of these components was 1:8:1. The composite was pressed onto an Al mesh current collector to form the electrode. The amount of the active material per electrode was *ca*. 2 mg in coin-type R2032. The area loading of the active material was ca. 1.7 mg/cm^2. A mixed solution of ethylene carbonate and diethyl carbonate (1:5, v/v) containing 1.0 M $LiPF_6$ was used as an electrolyte solution. A coin cell was fabricated by sandwiching a glass filter separator containing the electrolyte solution with the positive electrode and a metallic Li negative electrode under a low dew point (<–70°C) condition. The cell was charged up to 4.3 V with a current density of 40 mA g^{-1} and then discharged to 2.5 V with a current density of 100 mA g^{-1} at 30 °C.

Experimental procedures

Synthesis of compound 1 and 2

Compound **1**; $Pd(OAc)_2$ (21.2 mg, 0.094 mmol), P*t*Bu_3•HBF_4 (63.7 mg, 0.22 mmol), and Cs_2CO_3 (212.2 mg, 0.90 mmol) were placed in a 30-mL reaction flask under an argon atmosphere. 1,4-dioxane (10 mL) was added and the mixture was stirred for 10 min at 50 °C. Bz-TTF (51.2 mg, 0.20 mmol) and 4-bromotriphenylamine (194.8 mg, 0.60 mmol) were then added. The mixture was heated at 110 °C for 72 h, and then, the solvent was evaporated in vacuo. The residue was column chromatographed on silica gel by CS_2 and reprecipitated from CS_2/*n*hexane (1:15) to give **1** (118.0 mg, 0.16 mmol) as an orange powder in 80% yield. Compound **2**; $Pd(OAc)_2$ (20.3 mg, 0.090 mmol), P*t*Bu_3•HBF_4 (78.5 mg, 0.27 mmol), and Cs_2CO_3 (294.5 mg, 0.65 mmol) were placed in a 30-mL reaction flask under an argon atmosphere. 1,4-dioxane (4 mL) was added and the mixture was stirred for 10 min at 50 °C. Bz-TTF (40.7 mg, 0.16 mmo) and 4-bromo-*N*-methyl-*N*-phenylbenzenamine[4] (126.1 mg, 0.48 mmol) were then added. The mixture was heated at 110 °C for 3 days, and then, the solvent was evaporated in vacuo. The residue was column chromatographed on silica gel by CS_2 and reprecipitated from CS_2/*n*hexane (1:15) to give **2** (81.0 mg, 0.13 mmol) as an orange powder in 82% yield.

Spectral data of the products

1

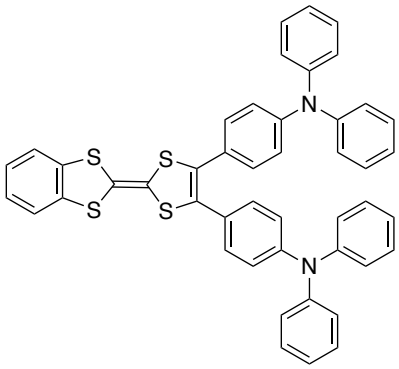

Yield: 80%; Orange powder; m.p. 248–249 ºC (decomposed); R_f = 0.28 (CS_2); ^{1}H NMR (acetone-d_6:CS_2 = 10:1, 400 MHz, 23 ºC, TMS) δ 6.86 (d, J = 8.8 Hz, 4H), 6.97–7.10 (m, 18H), 7.18–7.23 (m, 10H); ^{13}C NMR (C_6D_6:CS_2 = 10:1, 128 MHz, 24 ºC, TMS) δ 107.2, 111.8, 122.0, 122.4, 123.9, 125.3, 125.9, 126.2, 127.9, 129.8, 130.3, 137.8, 147.2, 147.8; IR (KBr) 3057, 3029, 1587, 1486, 1444, 1434, 1330, 1314, 1276, 753, 739, 694 cm^{-1}; HRMS (ESI): calcd. for $C_{46}H_{32}N_2S_4$ $[M]^+$: 740.1448; found: 740.1443.

2

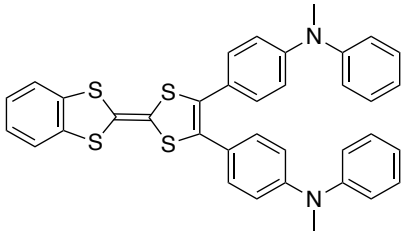

Yield: 82%; Yellow powder; m.p. 189–190 ºC; R_f = 0.28 (CS_2); ^{1}H NMR (acetone-d_6:CS_2 = 10:1, 400 MHz, 23 ºC, TMS) δ 3.31 (s, 6H), 6.76 (d, J = 8.8 Hz, 4H), 7.01–7.17 (m, 12H), 7.29–7.35 (m, 6H); ^{13}C NMR (C_6D_6:CS_2 = 10:1, 128 MHz, 24 ºC, TMS) δ 40.1, 106.4, 112.4, 117.1, 122.0, 123.9, 123.9, 125.9, 127.5, 128.4, 129.8, 130.3, 137.9, 148.2, 148.6; IR (KBr) 3031, 2871, 2811, 1606, 1588, 1508, 1492, 1340, 1254, 1191, 1178, 1119, 742, 698 cm^{-1}; HRMS (ESI): calcd. for $C_{36}H_{28}N_2S_4$ $[M]^+$: 616.1135; found: 616.1130; elemental analysis calcd. (%) for $C_{36}H_{28}N_2S_4$: C, 70.09; H, 4.58; N, 4.54, found: C, 69.80; H, 4.63; N, 4.50.

X-ray crystal structure analysis

Table S1. Crystal data of **1** and **2**.

	1	**2**
formula	$C_{46}H_{32}N_2S_4$	$C_{36}H_{28}N_2S_4$
T [K]	100	100
crystal system	triclinic	monoclinic
space group	P-1 (#2)	$P2_1/c$ (#14)
a [Å]	7.3839(2)	12.8261(4)
b [Å]	11.7705(3)	17.1559(5)
c [Å]	22.5226(6)	13.9852(4)
α [°]	79.201(2)	90.0000
β [°]	82.931(2)	105.543(3)
γ [°]	73.379(2)	90.0000
V [Å^3]	1837.46(9)	2964.81(16)
Z	2	4
D_{calc} [g cm^{-3}]	1.339	1.382
μ [mm^{-1}]	0.296	0.350
independent reflections	10650	8963
observed reflections [$I>2\sigma(I)$]	7894	6579
variable parameters	469	379
R_{int}	0.0538	0.0764
GOF on F^2	1.046	1.026
$R1$ [$I>2\sigma(I)$]	0.0521	0.0528
$wR2$ [$I>2\sigma(I)$]	0.1102	0.1054
$R1$ (all data)	0.0770	0.0825
$wR2$ (all data)	0.1217	0.1181
CCDC No.	2223557	2223558

(a)

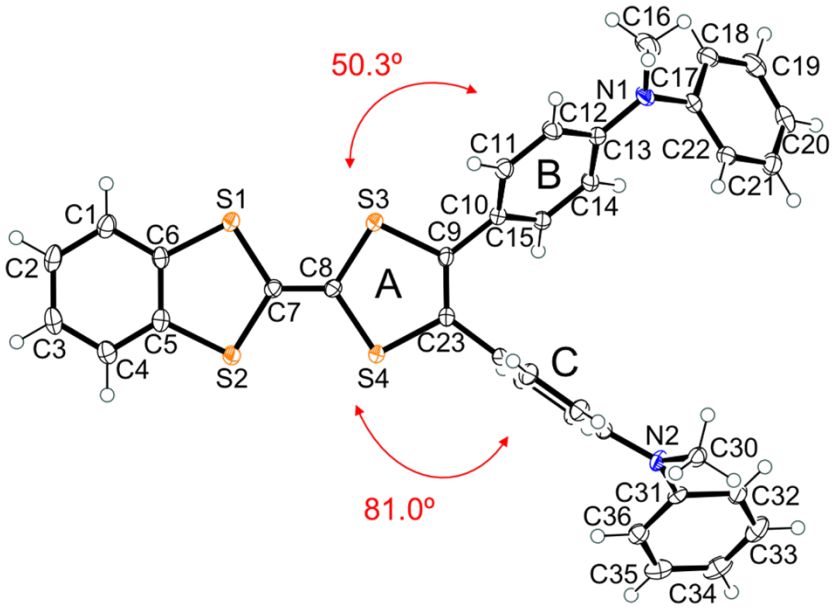

(b)

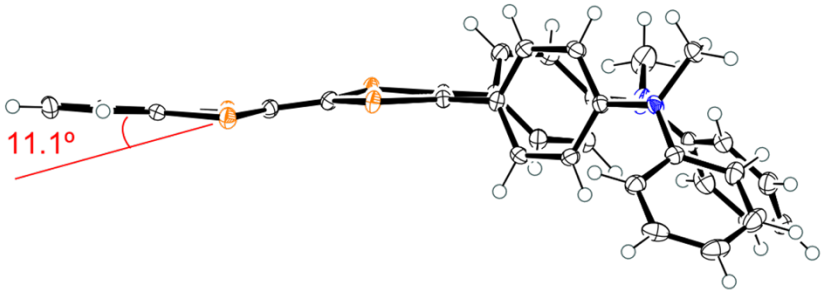

Fig. S1 (a) Top and (b) side views of ORTEP drawings for **2**. Ellipsoids displayed at 50% probability. The two TPA moieties on the 1,3-dithiole ring were twisted from the TTF core with dihedral angles of 50.3° (Plane A – Plane B) and 81.0° (Plane A – Plane C). The folding angle of the 1,3-dithiole ring along the S1–S2 axis being 11.1°.

(a)

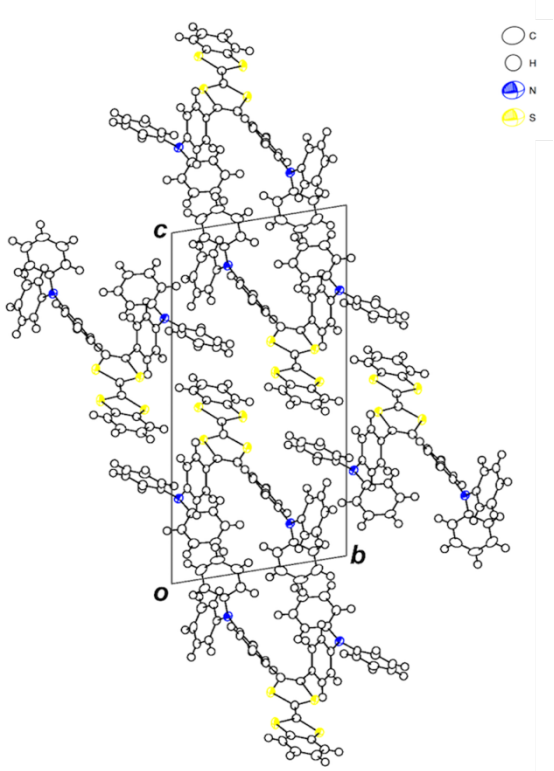

(b)

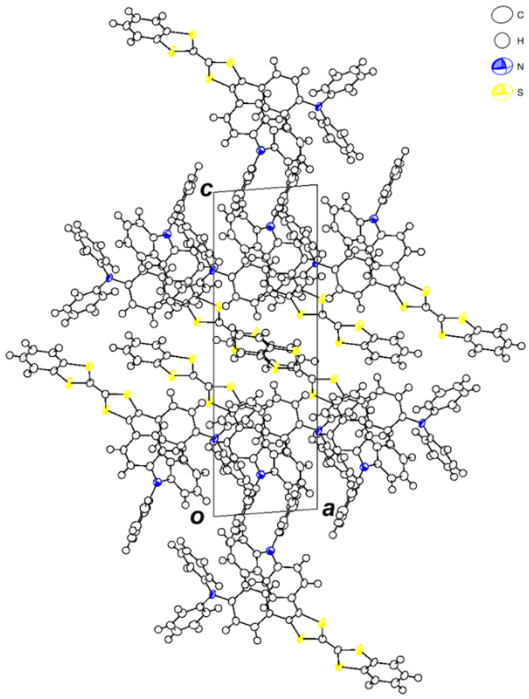

(c)

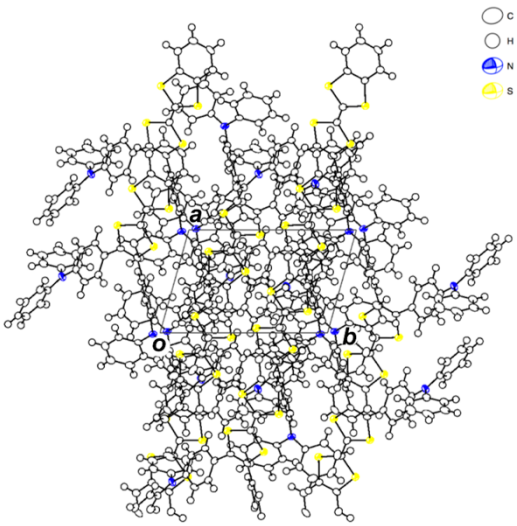

Fig. S2 Crystal structures of **1** viewed along (a) the *a* axis, (b) the *b* axis, and (c) the *c* axis.

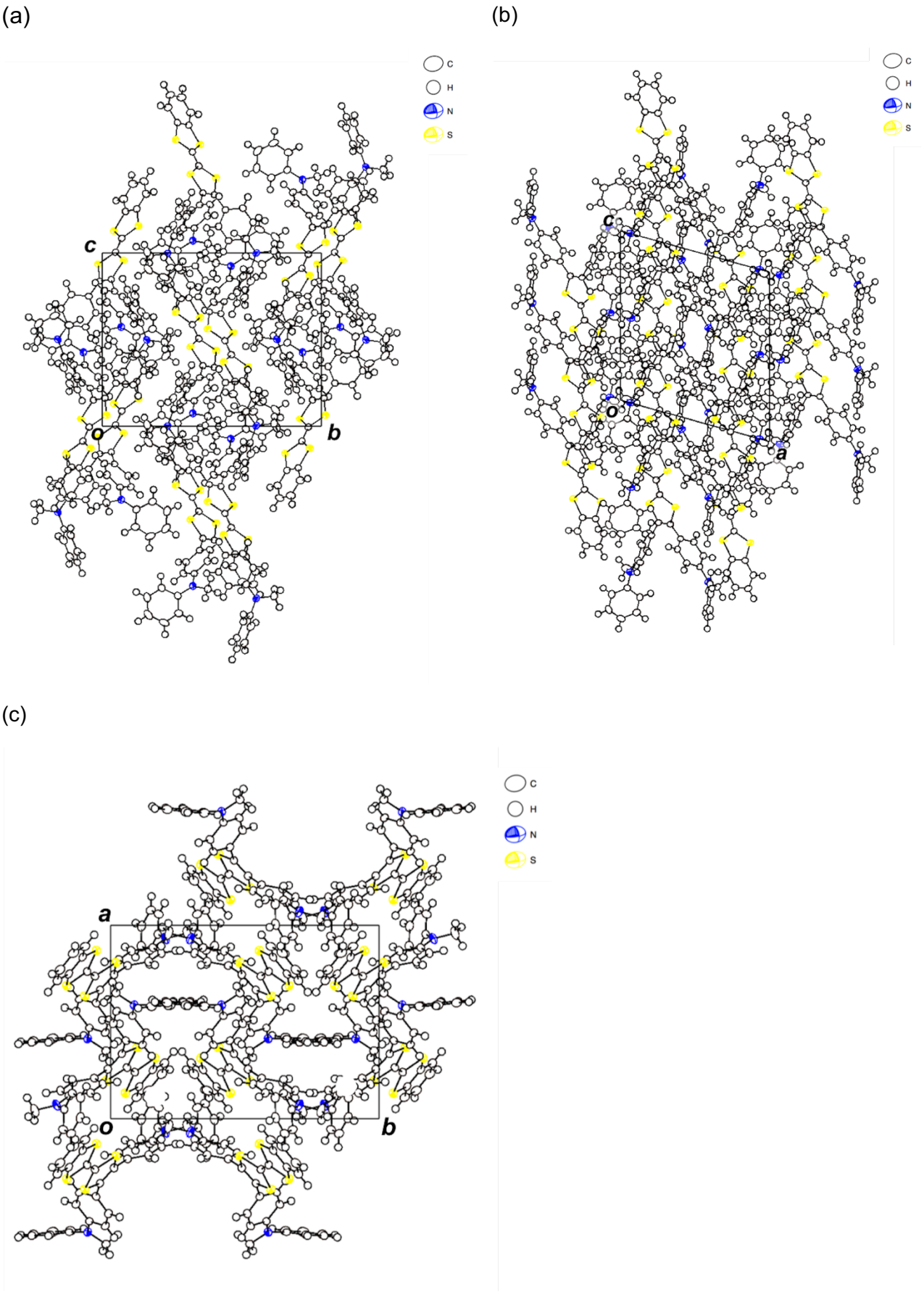

Fig. S3 Crystal structures of **2** viewed along (a) the *a* axis, (b) the *b* axis, and (c) the *c* axis.

(a)

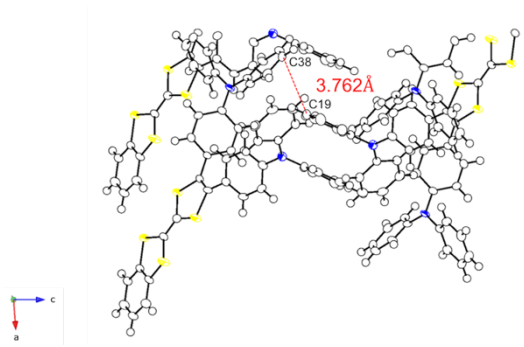

(b)

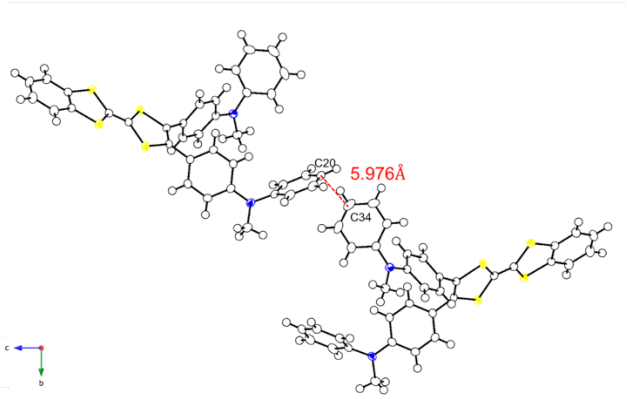

Fig. S4 (a) Crystal structures of **1**. The red dotted lines depicted the distance of reactive sites (C38···C19 = 3.762 Å). (b) Crystal structures of **2**. The red dotted lines depicted the distance of reactive sites (C34···C20 = 5.976 Å).

Powder XRD patterns

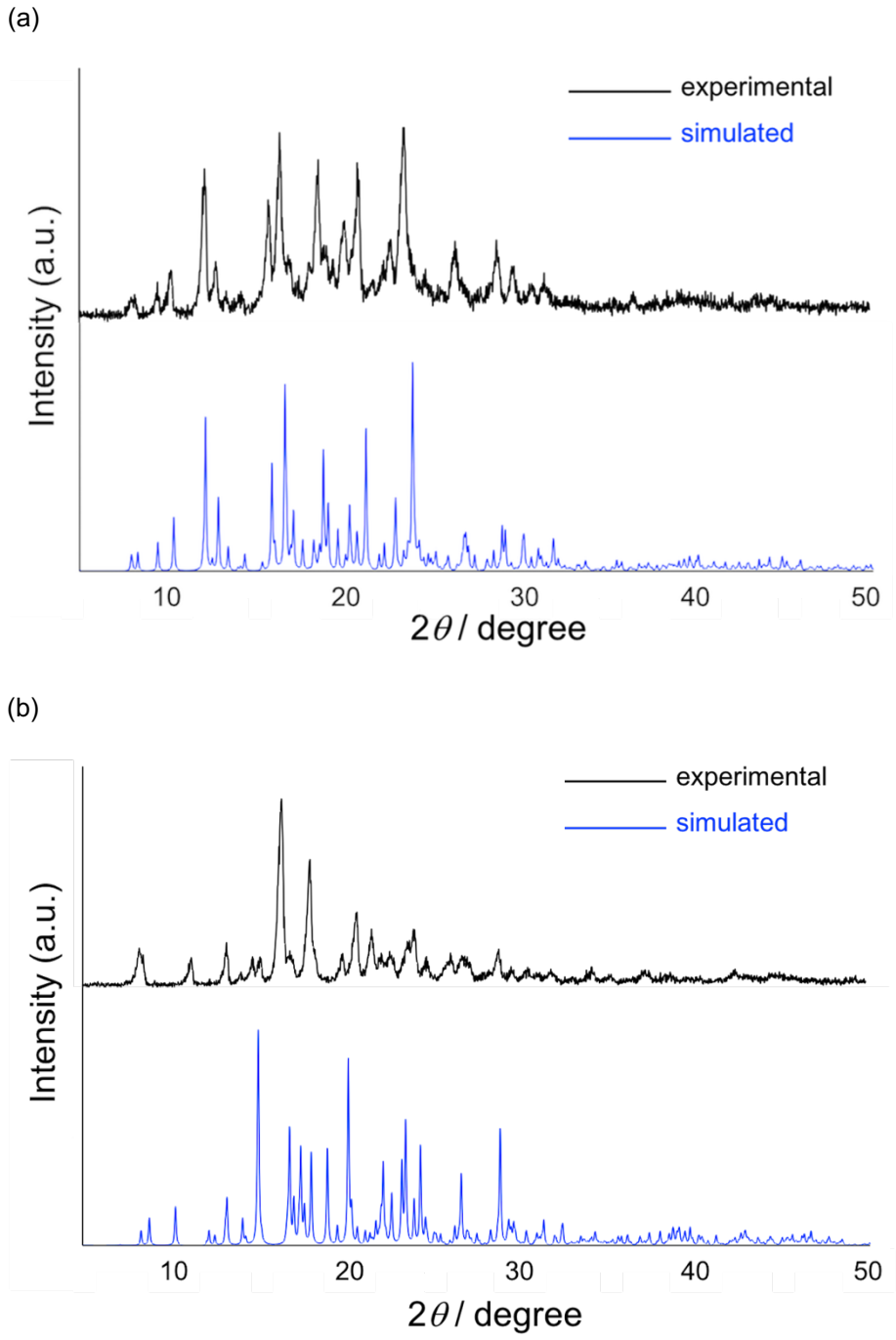

Fig. S5 Powder XRD pattern of (a) **1** and (b) **2**.

Cyclic voltammograms

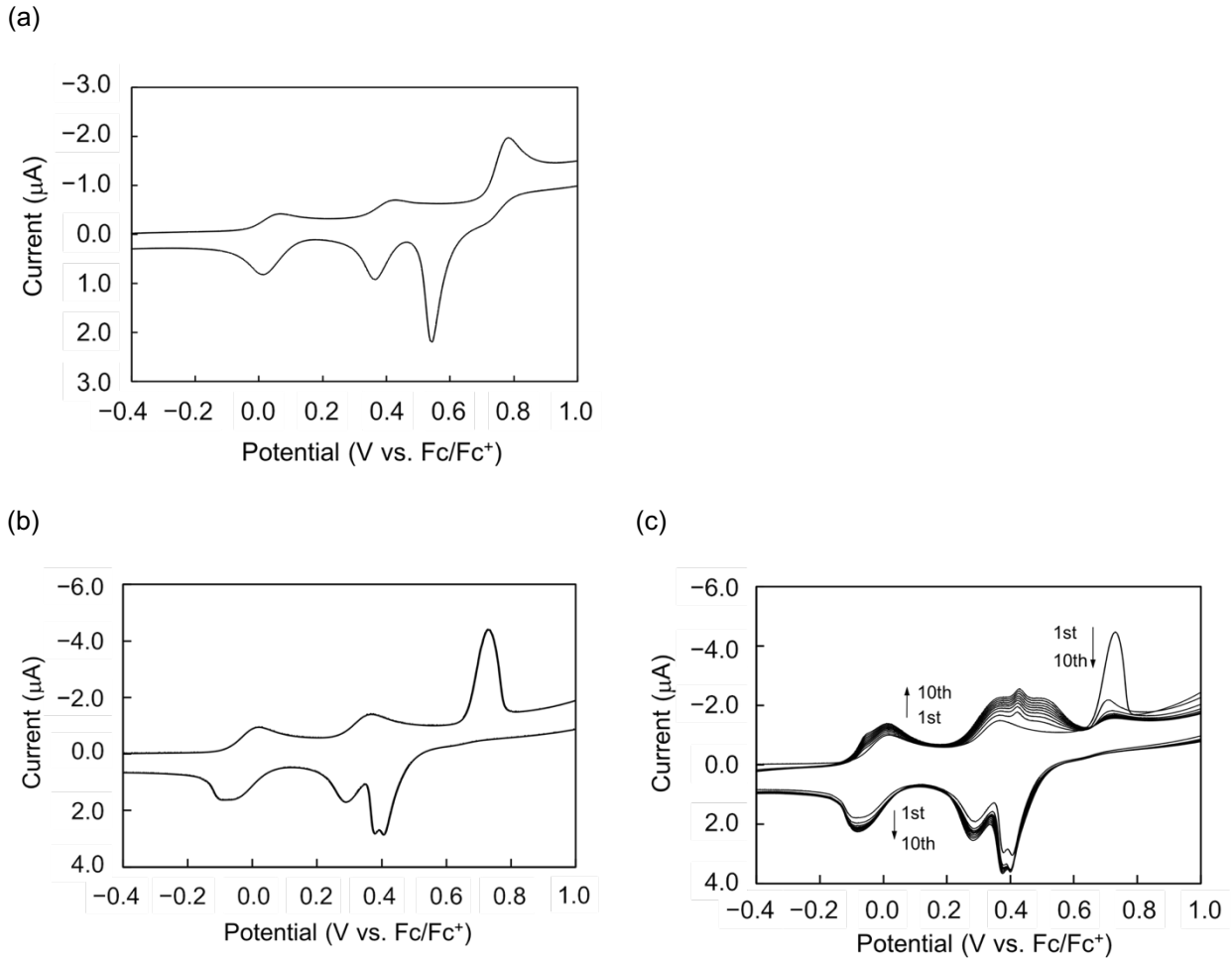

Fig. S6 Cyclic voltammograms of (a) **1** and (b) **2** (3.0 x 10^{-4} M) in a benzonitrile-carbon disulfide (1/1, v/v) solution containing 0.1 M $^{n}Bu_4NPF_6$ with the scan rate of 50 mV s^{-1}. (c) Repeating CV cycles of **2** with the scan rate of 50 mV s^{-1}.

Charge–discharge properties

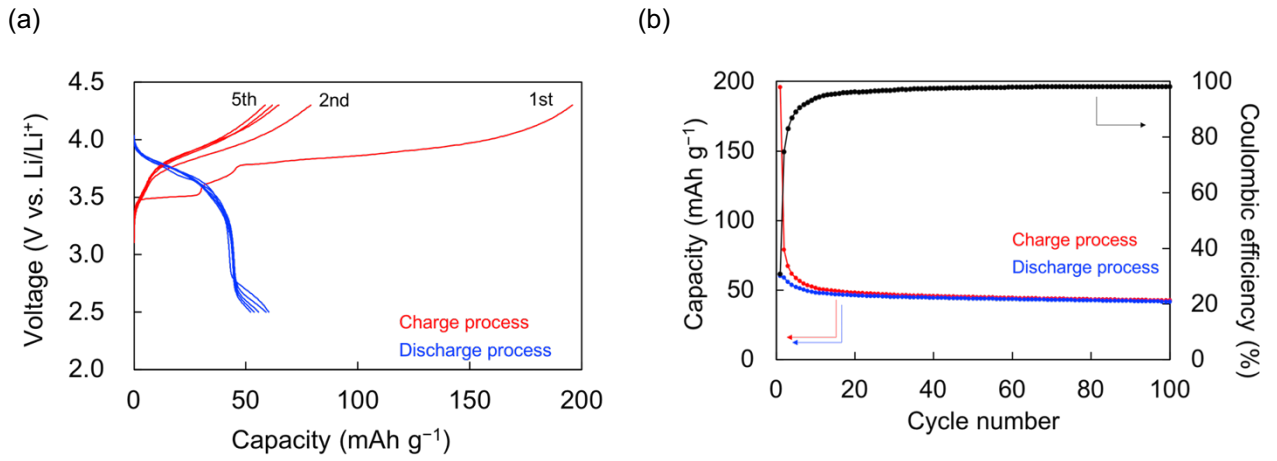

Fig. S7 (a) Galvanostatic charge–discharge curves of the **1**/Li cell at current densities of 40 mA g^{-1} (charge) and 100 mA g^{-1} (discharge). (b) Cyclic trend and Coulombic efficiency in the charge–discharge capacities of the **1**/Li cell. The electrode containing 50 wt% of **1**.

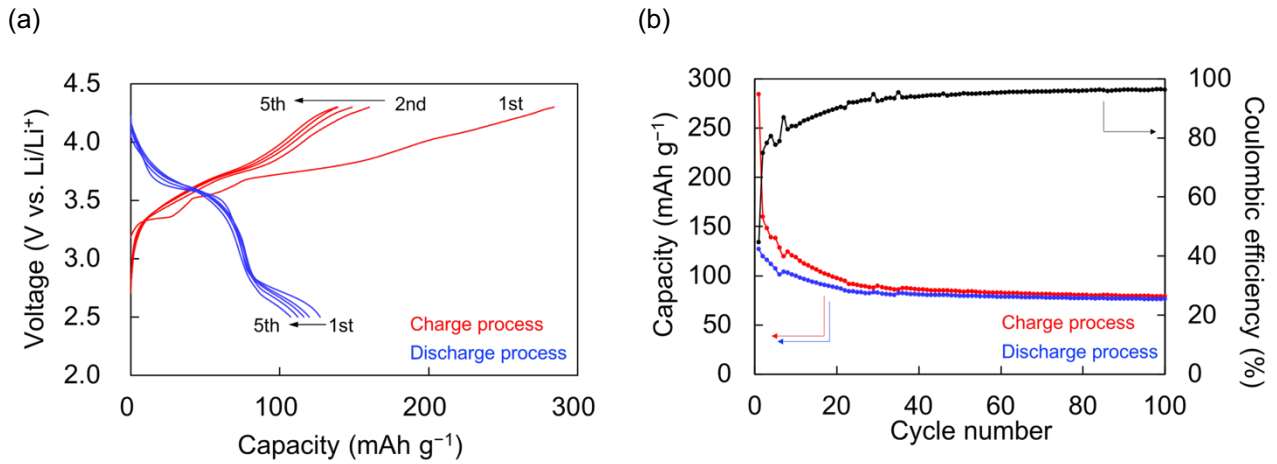

Fig. S8 (a) Galvanostatic charge–discharge curves of the **2**/Li cell at current densities of 40 mA g^{-1} (charge) and 100 mA g^{-1} (discharge). (b) Cyclic trend and Coulombic efficiency in the charge–discharge capacities of the **2**/Li cell.

Table S2. Charge–discharge parameters for the rechargeable batteries using **1** and **2**.

Compounds	**1**	**1**	**2**
The content of an active materials in a positive electrode (wt%)	10	50	10
1st Discharge capacity (mAh g^{-1})	132	60	127
Theoretical capacity for six-electron redox reaction (mAh g^{-1})	147	147	174
The average voltage for the first discharge (V (vs. Li/Li^+))	3.37	3.38	3.24
The energy density for the first discharge (mWh g^{-1})[a]	445	203	411

[a]The energy density is translated by the product of the capacity and the voltage.

The proposed redox and polymerization process of 1

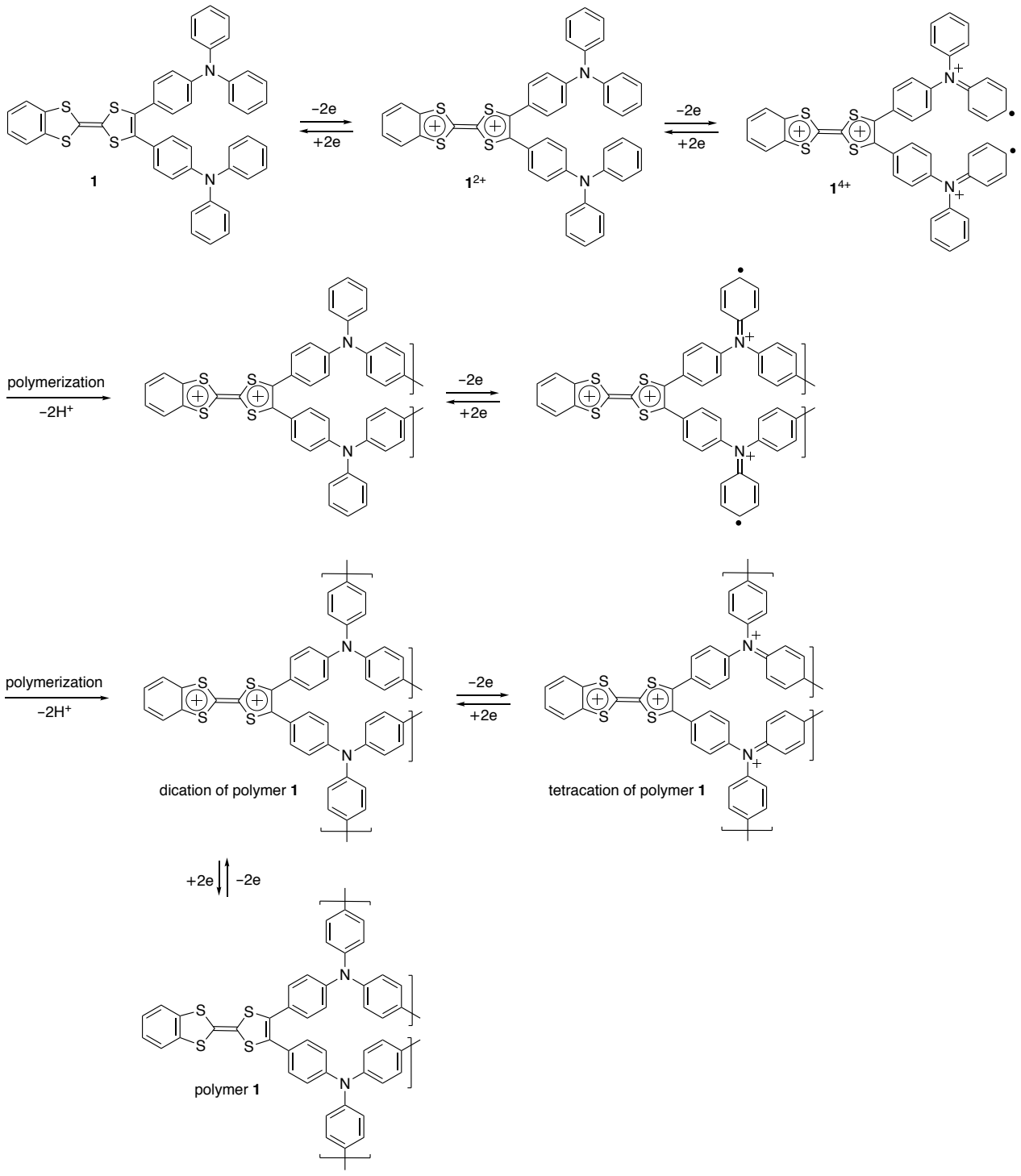

Scheme S1. The proposed redox and polymerization process of **1**.

Confirmation of polymerization

(a) (b)

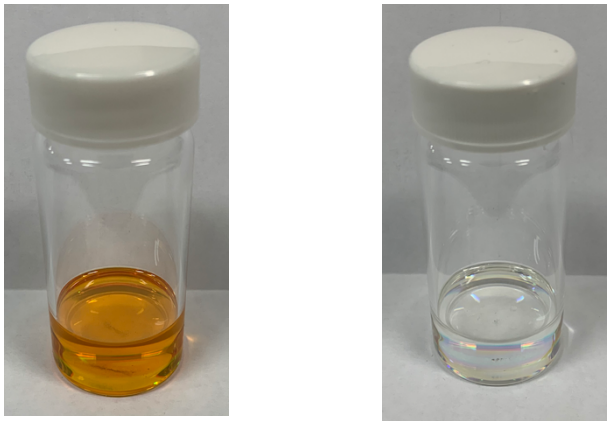

Fig. S9 Photos of (a) the orange solution obtained by washing the cell electrodes *before* charge-discharge processes using the 5 mL of carbon disulphide and (b) the colorless solution obtained by washing the cell electrodes *after* charge-discharge processes. The 5 mL of carbon disulfide was used for the washing.

(a)

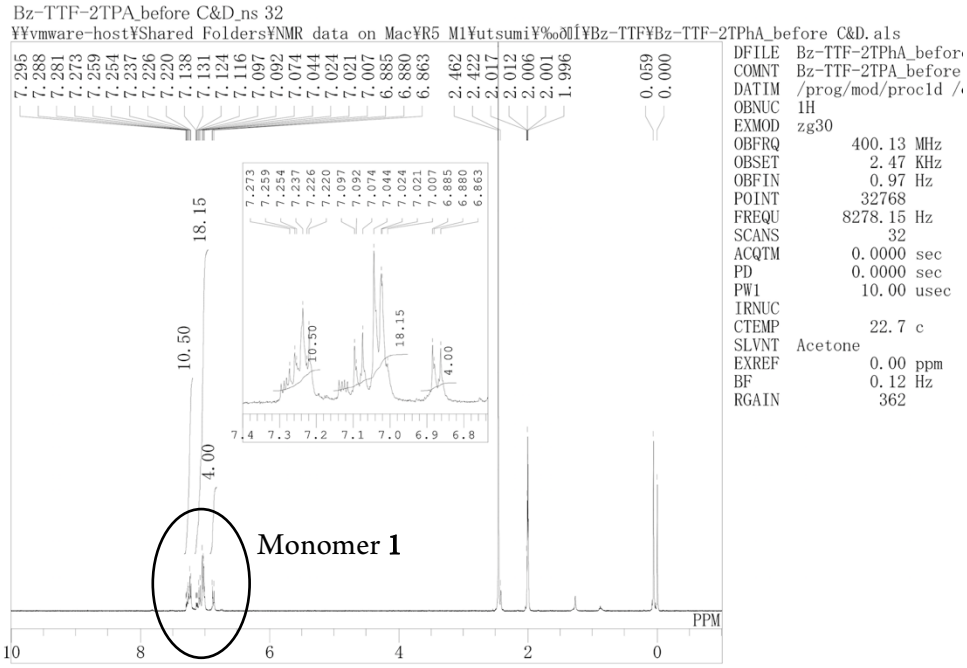

(b)

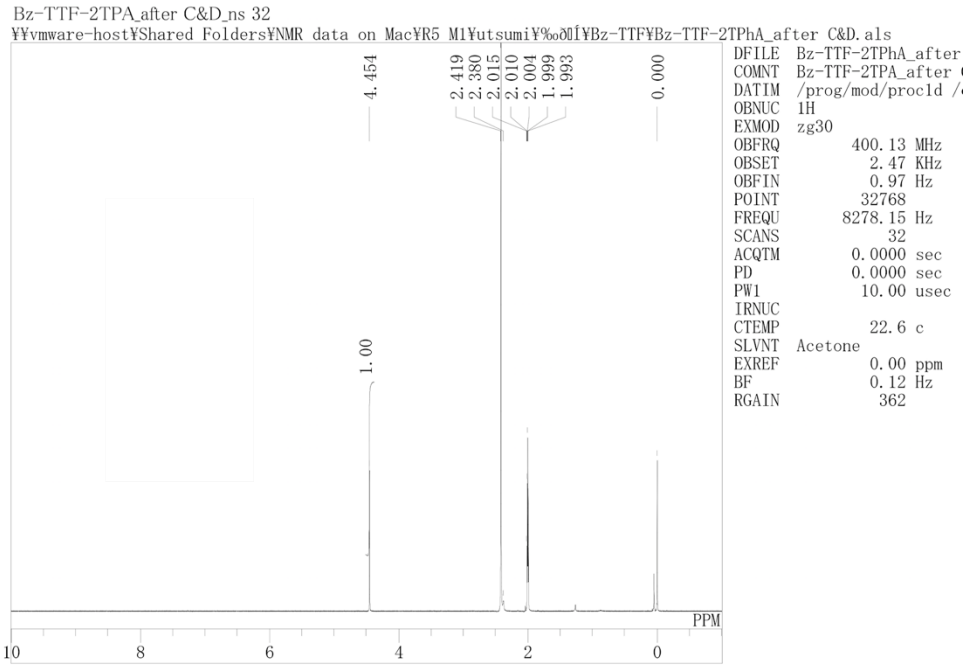

Fig. S10 ^{1}H NMR spectra of (a) residue from the orange solution (Fig. S9a) and (b) residue from the colorless solution (Fig. S9b) after evaporation of carbon disulfide.

NMR spectra

1 (^{1}H NMR)

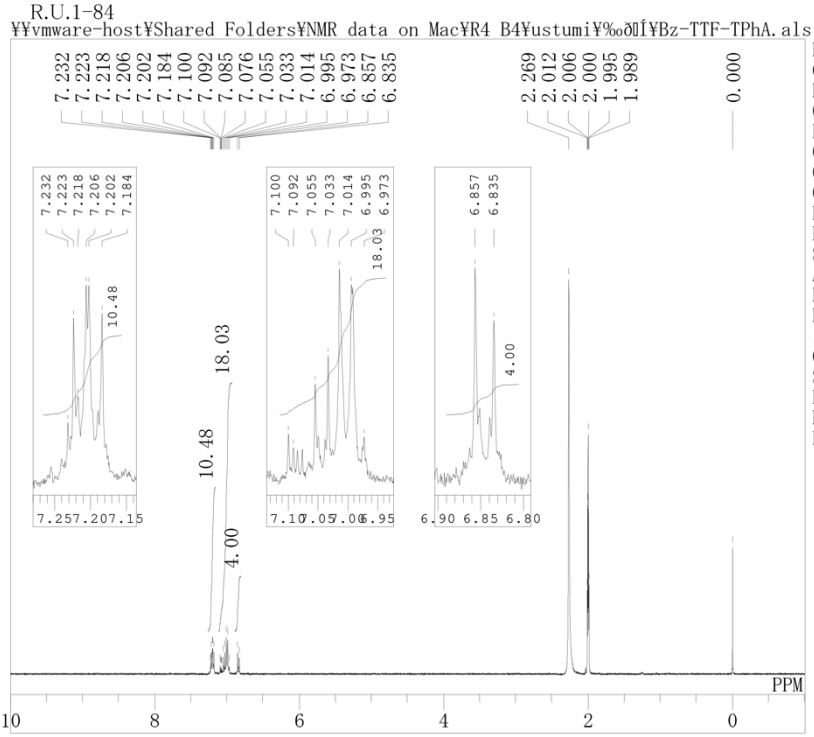

DFILE	Bz-TTF-TPhA.als
COMNT	R.U.1-84
DATIM	/prog/mod/proc1d /(
OBNUC	1H
EXMOD	zg30
OBFRQ	400.13 MHz
OBSET	2.47 KHz
OBFIN	0.97 Hz
POINT	32768
FREQU	8278.15 Hz
SCANS	16
ACQTM	0.0000 sec
PD	0.0000 sec
PW1	10.00 usec
IRNUC	
CTEMP	22.7 c
SLVNT	Acetone
EXREF	0.00 ppm
BF	0.12 Hz
RGAIN	362

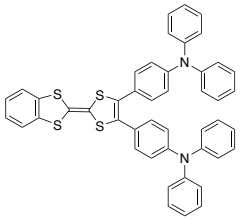

1 (^{13}C NMR)

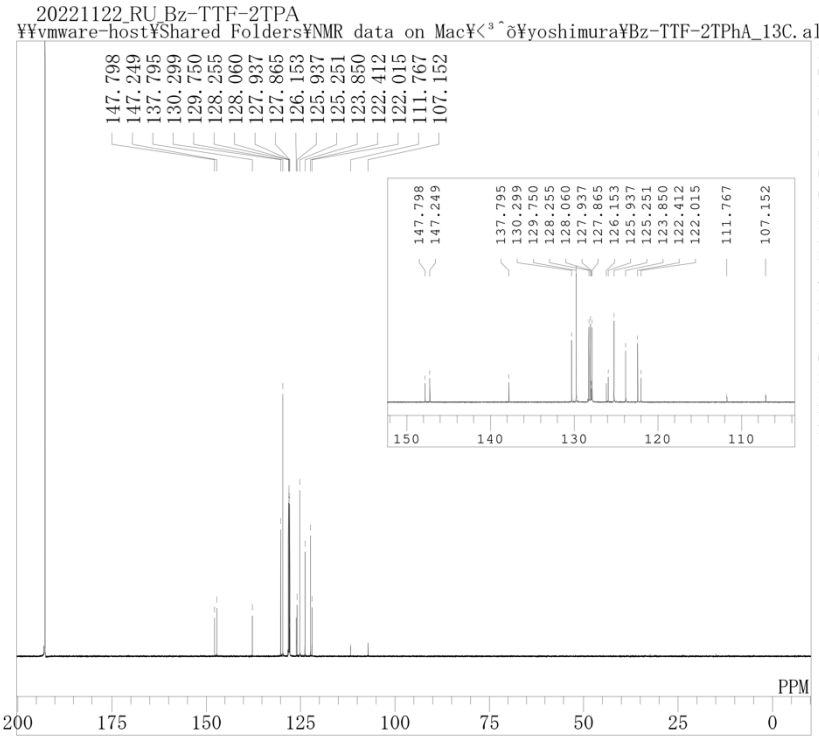

DFILE	Bz-TTF-2TPhA_13C.a
COMNT	20221122_RU_Bz-TTF-
DATIM	pSpin3.2¥prog¥mod¥
OBNUC	13C
EXMOD	zgpg30
OBFRQ	125.77 MHz
OBSET	5.39 KHz
OBFIN	3.22 Hz
POINT	32768
FREQU	29761.90 Hz
SCANS	1149
ACQTM	0.0000 sec
PD	0.0000 sec
PW1	10.00 usec
IRNUC	
CTEMP	23.8 c
SLVNT	C6D6
EXREF	128.06 ppm
BF	0.52 Hz
RGAIN	202

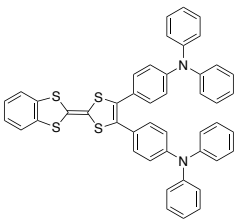

2 (^{1}H NMR)

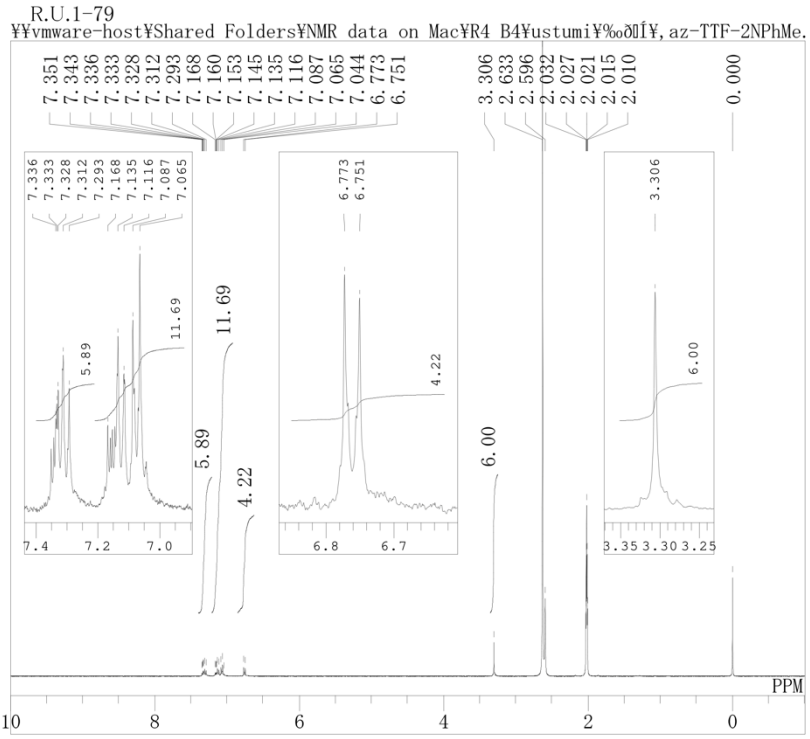

DFILE ,az-TTF-2NPhMe.als
COMNT R.U.1-79
DATIM /prog/mod/proc1d /
OBNUC 1H
EXMOD zg30
OBFRQ 400.13 MHz
OBSET 2.47 KHz
OBFIN 0.97 Hz
POINT 32768
FREQU 8278.15 Hz
SCANS 16
ACQTM 0.0000 sec
PD 0.0000 sec
PW1 10.00 usec
IRNUC
CTEMP 22.7 c
SLVNT Acetone
EXREF 0.00 ppm
BF 0.52 Hz
RGAIN 322

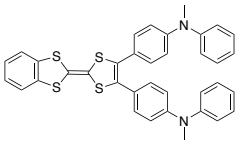

2 (^{13}C NMR)

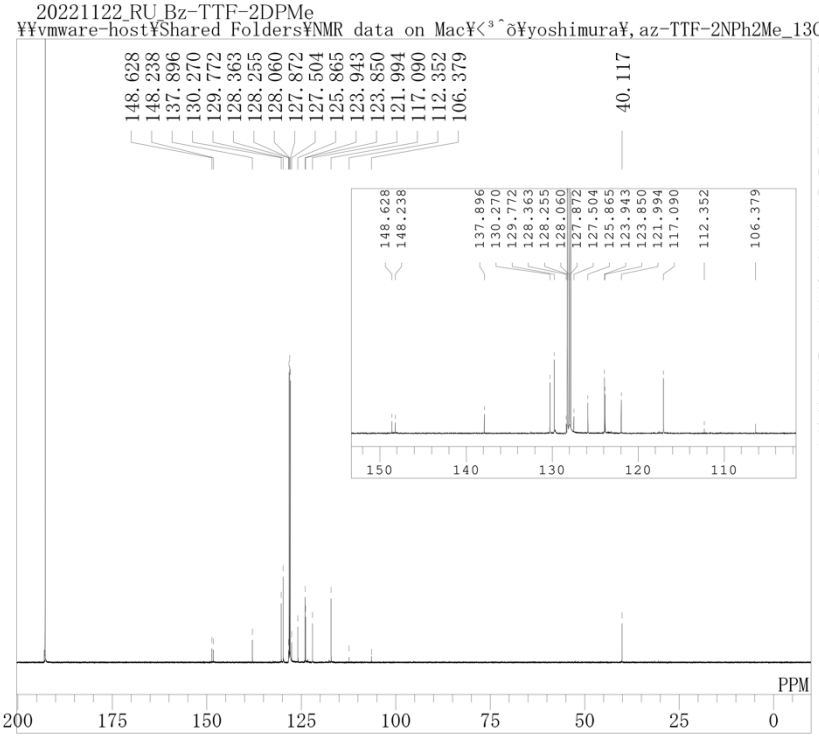

DFILE ,az-TTF-2NPh2Me_13
COMNT 20221122_RU_Bz-TTF
DATIM pSpin3.2¥prog¥mod¥
OBNUC 13C
EXMOD zgpg30
OBFRQ 125.77 MHz
OBSET 5.39 KHz
OBFIN 3.22 Hz
POINT 32768
FREQU 29761.90 Hz
SCANS 1388
ACQTM 0.0000 sec
PD 0.0000 sec
PW1 10.00 usec
IRNUC
CTEMP 23.8 c
SLVNT C6D6
EXREF 128.06 ppm
BF 0.52 Hz
RGAIN 202

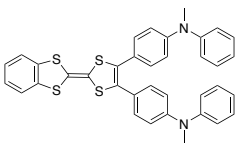

References

[1] *CrysAlisPro: Data Collection and Processing Software*, Rigaku Corporation, Toyko, Japan, 2015.

[2] *SHELXT*: Sheldrick, G. M. *Acta Cryst.* 2015, **A71**, 3–8.

[3] *SHELXL*: Sheldrick, G. M. *Acta Cryst.* 2015, **C71**, 3–8.

[4] S. S. Bhojgude, T. Kaicharla and A. T. Biju, *Org. Lett.,* 2013, **15**, 5452.